Effect of Oblate Sun on Planetary Orbits

Summer Project Report

Dhruv Aryan, Esha Sajjanhar

Mentors

Prof. Bikram Phookun

Philip Cherian

Department of Physics

Ashoka University

September 25, 2022

Abstract

Newtonian gravitation relies upon the assumption of a uniform mass distribution. Deviations from such ideal conditions are common and they necessitate an alternate theoretical framework. One such framework which provides an expression for the potential of an oblate star is explored here. We explore the consequences of stellar oblateness on planetary orbits in terms of the rate of perihelion precession. We use the velocity verlet algorithm to solve the two-body problem for a planet going around an oblate sun. This model is then used to find a numerical solution for the rate of angular precession of perihelion. This allows us to verify that the rate of precession is directly proportional to the magnitude of solar oblateness given by gravitational quadrupole moment, J_2. This is then compared with an analytical prediction.

Contents

Introduction

For centuries, physicists and astronomers have been fascinated by the motion of planets and stars. Newton's account of this motion is still considered a good approximation. However, this model relies on the assumption that a celestial body such as a star can be approximated to a point mass. This assumption fails when the body in question does not have a uniform mass distribution.

Stars like the Sun are not perfectly spherical and are instead somewhat flattened. This deviation from a spherical shape is measured as stellar oblateness given by the gravitational quadrupole moment, J_2. The problem of solar oblateness and its effects on planetary orbits is very interesting and has widespread possible applications. Any stellar processes that affect the stellar surface affect the apparent shape of the star. For the Sun, this breaks the assumption of a perfectly uniform mass distribution.

In this paper, we explore the effects of solar oblateness on planetary orbits, specifically with respect to prograde precession of the perihelion. In Section II we describe the model in question which comprises a planet in orbit around an oblate star and the theoretical framework used to analyse the same. In Section III we describe the computational techniques required to implement this model numerically. In Section IV we describe the results obtained through the numerical model and their agreement with theoretical solutions. Section V is dedicated to a discussion of computational accuracy and error analysis. Section VI further explores the implications of these results and potential extensions to the model.

Model

Spherical Sun

From Newton's Law of Gravitation, we know that the equation of motion of a planet at position $\mathbf{r}$ in the gravitational field of a star with mass M is given by

$$\frac{d^2\mathbf{r}}{dt^2} = -\frac{GM}{r^3}\mathbf{r}\,, \tag{1}$$

where G is the universal gravitational constant ($\approx 6.67\,\mathrm{m^3 kg^{-1} s^{-2}}$).

This equation gives the acceleration experienced by the planet along each axis and thereby allows us to chart its trajectory. However, this model does not take into account deviations

from a uniform mass distribution. Thus, we must introduce other terms to deal with oblateness.

Oblate Sun

The internal dynamics of a star lead to disturbances on its surface and thus also affect its shape. Solar shape is understood using three main factors: gravitation, internal rotation and changing magnetic field. In this paper, we use the gravitational quadrupole moment, J_2, as the measure for solar oblateness.

The potential of an oblate star can be expressed as an infinite sum. Keeping only the monopole and quadrupole terms, the gravitational potential of an oblate star with mass M, radius R and oblateness J_2 is given by

$$\phi(r,\theta) = -\frac{GM}{r}\left(P_0(\cos\theta) - J_2\frac{R^2}{r^2}P_2(\cos\theta)\right), \tag{2}$$

where $P_n(\cos\theta)$ are Legendre polynomials.[1] We can use this to get the equation of motion of a planet at position $\mathbf{r}$ in the gravitational field of an oblate star, given by

$$\frac{d^2\mathbf{r}}{dt^2} = -\frac{GM}{r^3}\left(1 - 3J_2P_2(\cos\theta)\frac{R^2}{r^2} + 3J_2\sin^2\frac{R^2}{r^2}\right)\mathbf{r}. \tag{3}$$

In cartesian coordinates, this would give us the following set of equations for the acceleration of the planet:

$$a_x = -\frac{GM}{r^3}\left(1 - 3J_2P_2(\cos\theta)\frac{R^2}{r^2} + 3J_2\sin^2\theta\frac{R^2}{r^2}\right)\mathbf{x}, \tag{4}$$

$$a_y = -\frac{GM}{r^3}\left(1 - 3J_2P_2(\cos\theta)\frac{R^2}{r^2} + 3J_2\cos^2\theta\frac{R^2}{r^2}\right)\mathbf{y}. \tag{5}$$

It is conceivable that introducing oblateness as above would change the nature of the planetary orbit. This is indeed observed to be the case. Fig(1a) below shows the orbit of a hypothetical Mercury-like planet (planet P, see **Initial Conditions** (p.4)) around a perfectly spherical star. Fig(1b) shows the orbit of the same planet around an oblate star.

[1] Legendre polynomials provide an expansion for a $1/r$ potential as a converging series.

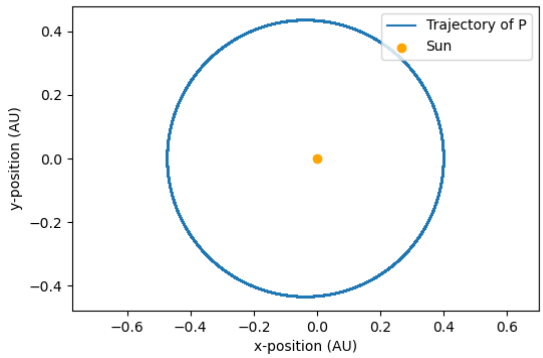

(a) The planetary orbit observed for solar oblateness $J_2 = 0$

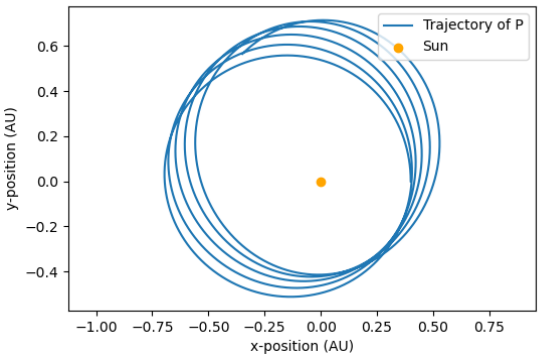

(b) The planetary orbit observed for solar oblateness $J_2 = 700$

Figure 1

In comparing the two figures, we find that the non-precessing orbit in Fig(1a) behaves as a precessing ellipse in Fig(1b). To model this effect of an oblate sun, we can imagine a precessing elliptical orbit to be a circular orbit with a small radial oscillation. Thus, such an orbit would have a circular and a radial frequency which would together determine its precession.

To supplement this model of the orbit, we obtain two factors that are closely related to the periodicity of the orbit from the monopole and quadrupole terms of the potential. These are,

$$\kappa^2 = \frac{GM}{r^3}\left(1 - \frac{3}{2}J_2\frac{R^2}{r^2}\right), \tag{6}$$

$$\Omega^2 = \frac{GM}{r^3}\left(1 + \frac{3}{2}J_2\frac{R^2}{r^2}\right), \tag{7}$$

where $2\pi/\Omega$ is the time taken for one rotation and $2\pi/\kappa$ is the time between successive approaches to aphelion. Thus, $\Omega - \kappa$ represents the difference between the period of rotation and radial oscillation. It is this difference which results in a prograde precession of the perihelion of the orbit. The magnitude of the perihelion shift per unit time is given by,

$$\Omega - \kappa = \frac{3}{2}J_2\frac{R^2}{r^2}. \tag{8}$$

Initial Conditions

We consider a Mercury-like planet P with mass $m = 3.3 \times 10^{23}$kg at a distance 0.4AU from a Sun-like star S, where $1\text{AU} = 1.49 \times 10^{11}$m. The model is independent of the

mass of the planet. Since the objective of this model is to consider the effects of solar oblateness alone, we disregard planetary oblateness and assume that the planet has a uniform mass distribution which can be approximated to a point mass at its centre of gravity.

We consider a star of mass $M = 2 \times 10^{30}$kg with a radius of $R = 6.8 \times 10^8$ m in the spherical case, and an equivalent average radius in the oblate case. We consider the time period of the revolution of planet P around this star to be 88 days. Given these conditions, the initial velocity of P is $49,252.7$ ms^{-1}. This is directed entirely along the y-axis.

Method

Velocity Verlet Integration

In order to track the trajectory of the planet, we used the velocity verlet algorithm as a numerical integrator. This algorithm uses (4), (5) in order to find the acceleration of a body at each time step and thus evaluates its position and velocity at these time steps. This position and velocity data can be used to track the motion of the body in question.

Velocity verlet is similar to the leap frog integration algorithm, with the exception that velocity and position are calculated at the same value of the time variable. The integrator relies upon the following equations:

$$x(t + \Delta t) = x(t) + v(t)\Delta t + \frac{1}{2}a(t)\Delta t^2 \tag{9}$$

$$v(t + \Delta t) = v(t) + \frac{a(t) + a(t + \Delta t)}{2}\Delta t \tag{10}$$

Errors introduced by velocity verlet are of the order of $(\Delta t)^2$ whereas those introduced by leapfrog are of the order of Δt. Thus, we used velocity verlet for higher accuracy and to limit numerical errors.

Numerical Solution Algorithm

As described above, the velocity verlet integrator was used to plot the trajectory of planet P around stars A and B. Using the position and velocity data thus obtained, it is possible to analyse the changes in the orbit caused by the introduction of solar oblateness.

Precession of the planetary orbit is the most tangible consequence of solar oblateness and this is the consequence of oblateness explored here.

To find the angular precession rate of the perihelion as a function of oblateness numerically, we follow the following algorithm. For a given value of oblateness, we first plot the distance between the star and the planet (r) as a function of time (t) as shown in Fig(2). We then identify the perihelia as the minima of this graph using the `find_peaks` function from the `sci_pi` library. This function compares adjacent values of the array in order to identify minima with high accuracy.

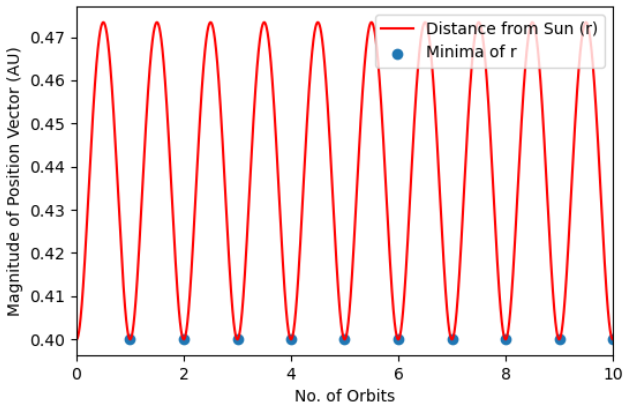

Figure 2: The distance between the planet and the star as a function of time and its minima for solar oblateness $J_2 = 1$

We use these minima to obtain the angle θ formed between the line joining the planet and the sun and the reference (y-) axis in our coordinate system at these points. The slope of the line of best fit for this graph is calculated. An example of the line of best fit plotted for this data can be seen in Fig(4). When we do this for the case of $J_2 = 0$, we get a very small but non-zero slope (shown in Fig(3)). This is an artifact of the computational solution. In order to increase accuracy of the numerical solution for non-zero values of J_2, we subtract this small slope from the slope obtained from every other value of J_2.

Further, using equation (8) in conjunction with the numerical data, it is possible to obtain an analytical value for the angular rate of precession of the planetary perihelion. This provides a point of comparison for the numerical precession rate obtained as described above.

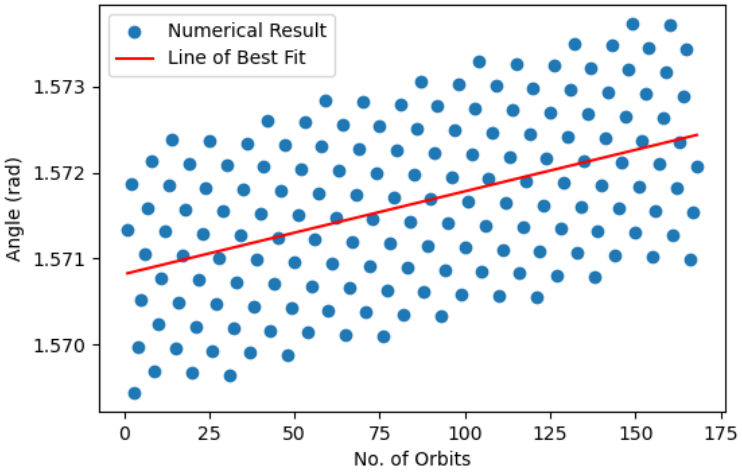

Figure 3: The angular position of the perihelion of the planet's orbit as a function of time for solar oblateness $J_2 = 0$

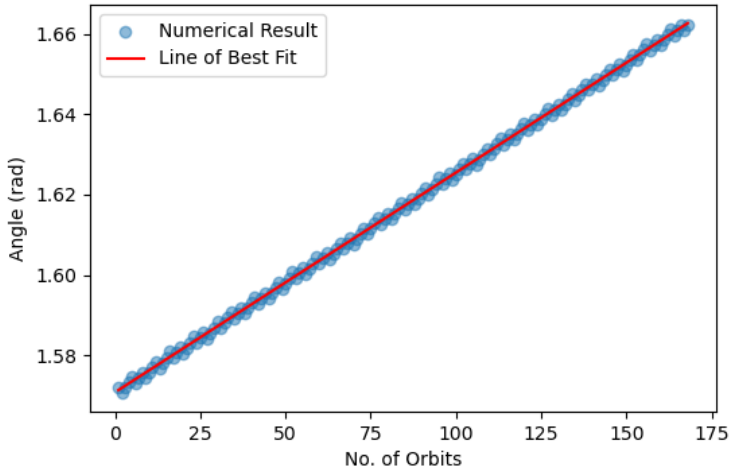

Figure 4: The angular position of the perihelion of the planet's orbit as a function of time for solar oblateness $J_2 = 1$

Results

Oblateness and Precession

We can see that oblateness of the star does in fact induce precession in the orbits of planets from the graph in Fig(5). It is observed that the angle at the perihelion precesses with time and the magnitude of this precession depends on the oblateness of the sun.

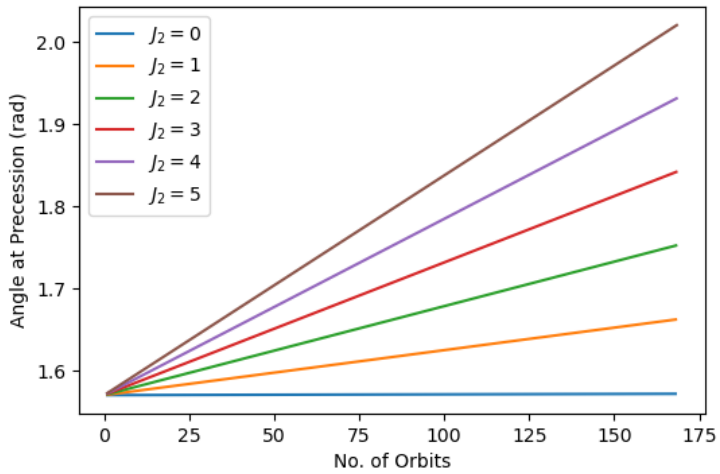

Figure 5: Angle (θ) at perihelion versus time at perihelion for various values of J_2

The slope of this graph is higher for higher values of J_2 indicating that the rate of perihelion precession is proportional to the oblateness of the sun.

Precession Rate and Oblateness

An analytical value for the rate of perihelion precession for a given value of J_2 is obtained using eq(8). A numerical value for the same is obtained using the algorithm described above. Comparing the two over a range of values for solar oblateness, we find a peculiar relationship between the slopes of the two graphs. It is found that the two solutions disagree by a consistent factor, i.e. the ratio between the two solutions remains approximately constant for each value of J_2 as in Fig(6a). We found that the missing factor is very well approximated by π. Upon multiplying the analytical solution by π we discover that the two solutions show almost perfect agreement, as shown in Fig(6b) below.

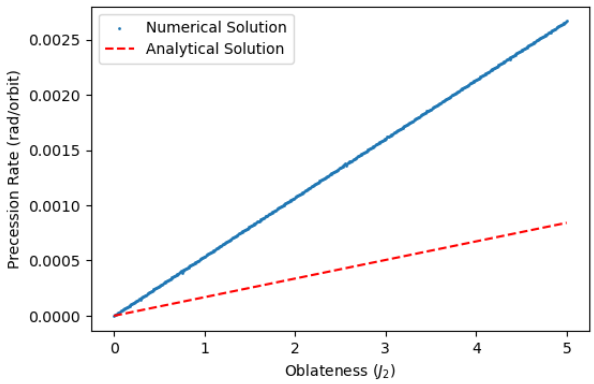

(a) Comparing the analytical and numerical values for rate of perihelion precession against value of oblateness J_2 for $0 \geq J_2 \geq 5$

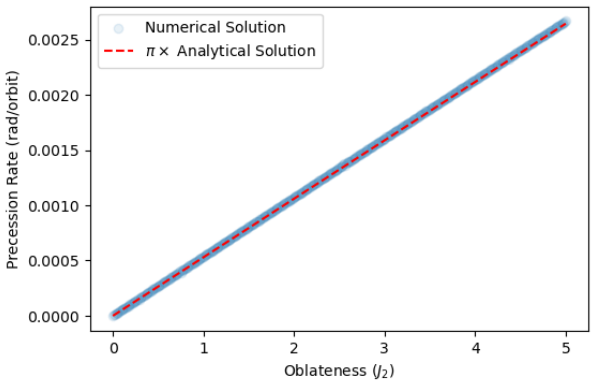

(b) Comparing $\pi\times$ analytical solution with numerical solution for rate of perihelion precession for $0 \geq J_2 \geq 5$

Figure 6

We can test the consistency of this factor by individually varying the parameters upon which the analytical solution depends. From Eq(8), we can see that these parameters are the squre of the radius of the sun and the inverse square of the initial distance of the planet from the sun. We first vary the radius of the sun for $J_2 = 1$ and distance between the planet and the sun, $r = 0.4$AU in Fig(7a). Once again, the solutions appear to vary by a consistent factor. Upon multiplying the analytical solution by a factor of π, we find that the two solutions agree within a reasonable error margin as shown in Fig(7b).

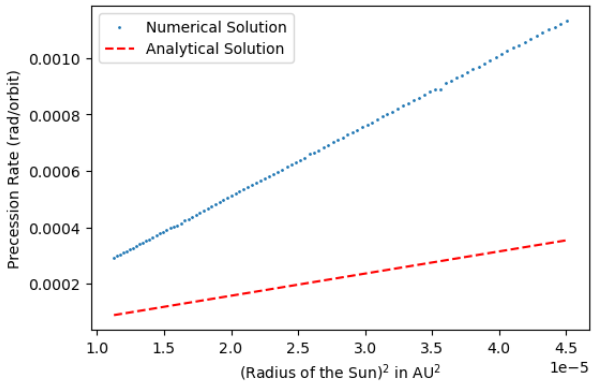

(a) Analytical and Numerical solutions for rate of precession for various values of R^2

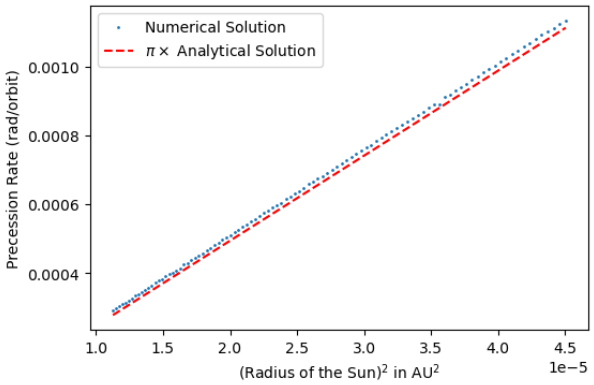

(b) $\pi\times$ analytical solution compared with numerical solution for rate of precession for various values of R^2

Figure 7

We now vary the distance between the planet and the sun, r, for fixed oblateness $J_2 = 1$ and fixed radius of the sun $R = 6.9 \times 10^8$m. The relationship between the analytical and numerical solutions for various values of $1/r^2$ is shown in Fig(8a). Once again, the

solutions appear to vary by a consistent factor. Upon multiplying the analytical solution by a factor of π, we find that the two solutions agree within a reasonable error margin as in Fig(8b).

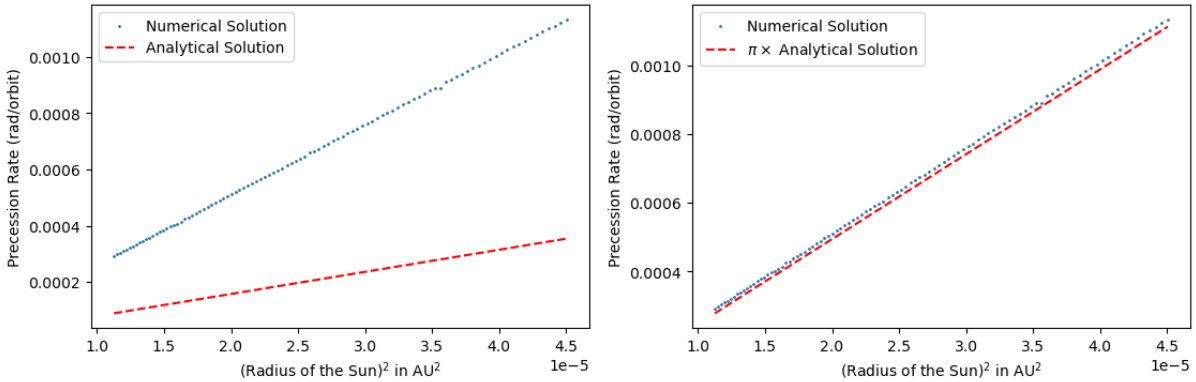

(a) Analytical and Numerical solutions for rate of precession for various values of $1/r^2$

(b) $\pi\times$ analytical solution compared with numerical solution for rate of precession for various values of $1/r^2$

Figure 8

Thus, this disagreement by a factor of π appears consistently in our results. That the factor persists even upon varying different parameters would suggest that this result is not an artefact of the results of numerical integration. It appears to be a fundamental inconsistency between our numerical and analytical solutions. This inconsistency remains as yet unexplained.

Testing Computational Accuracy

We know that the total energy and angular momentum of the system must be conserved in order to preserve its physical reliability. Thus, testing the conservation of these quantities in the simulated model provides an estimate of the accuracy of the computational methods used therein. Below, we have shown the total energy and angular momentum of the system as a fraction of its mean value against time.

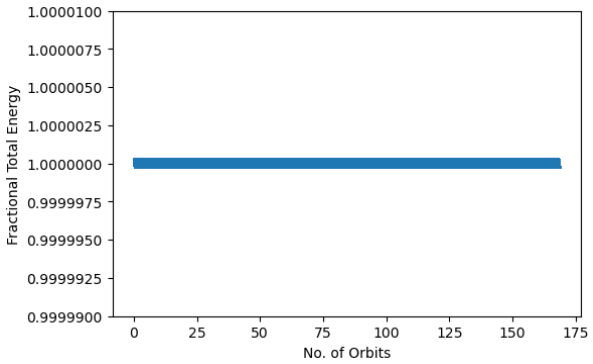

(a) Variation in total energy of the system as a fraction of mean total energy against time for $J_2 = 0$

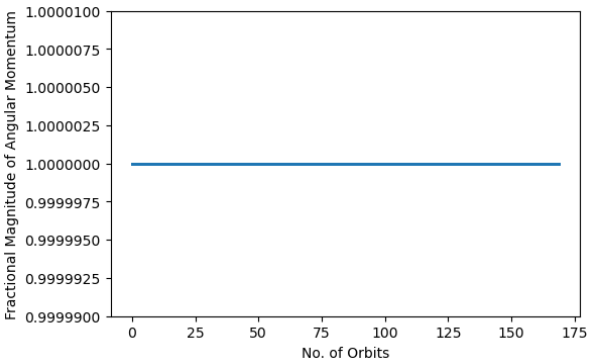

(b) Variation in total angular momentum of the system as a fraction of mean total angular momentum against time for $J_2 = 0$

Figure 9

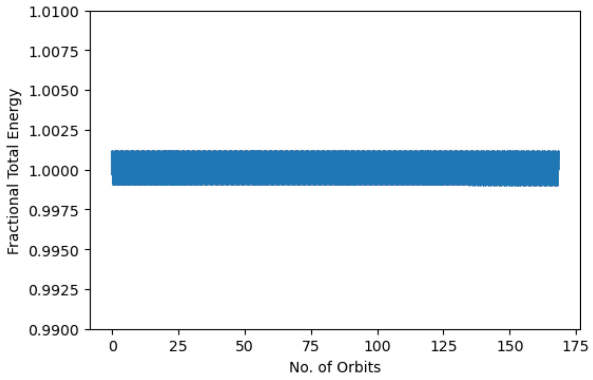

(a) Variation in total energy of the system as a fraction of mean total energy against time for $J_2 = 5$

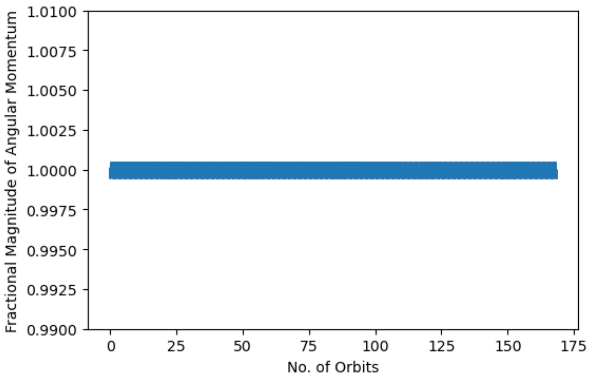

(b) Variation in total angular momentum of the system as a fraction of mean total angular momentum against time for $J_2 = 5$

Figure 10

In the above graphs, we can see that there is minimal variation in total energy and angular momentum in the system. This verifies the internal consistencies of the physical system.

Error Analysis

Equations (9) and (10) tell us that the error of both displacement r and velocity v are of the order of $(\Delta t)^2$. Hence, $\Delta r = O(\Delta t^2)$ and $\Delta v = O(\Delta t^2)$. We know that the time period T of the orbit is given by

$$T = \frac{2\pi r}{v} \tag{11}$$

Thus, we get

$$\frac{\Delta T}{T} = \sqrt{\left(\frac{\Delta r}{r}\right)^2 + \left(\frac{\Delta v}{v}\right)^2} \tag{12}$$

On putting in values of Δt, r and v, we get

$$\frac{\Delta T}{T} \approx \sqrt{\left(\frac{3600^2}{10^{11}}\right)^2 + \left(\frac{3600^2}{10^4}\right)^2} \tag{13}$$

Thus, putting the value of T as 88 days, we get that $\Delta T = 31.68$ days. Therefore, $T = 88 \pm 32$ days. The time period obtained numerically is roughly 104 days, which is within the allowed error range.

Conclusion

It was found that the oblateness of the sun introduces perihelion precession to planetary orbits, and the rate of such precession is proportional to the oblateness of the sun. Eq(8) allows us to compute an analytical value for the rate of this precession, and we found that our algorithm leads to a similar value for this rate which varies from the former by an approximate factor of π.

Discussion

Our work on the perihelion precession due to solar oblateness needs to be extended further in order to identify the origin of the confounding factor of π. The source of this factor almost certainly lies in the manner of evaluation of the rate of perihelion precession, rather than in numerical or computational errors in the construction of the model itself as indicated by the internal consistency of the model. Further, it can be reasoned that this error likely arises out of a disagreement in the manner in which angular frequencies are evaluated in either case.

It is also possible to modify the model used here to evaluate the variation in the value of acceleration due to gravity, g, on the surface of a planet due to planetary oblateness. Such a model would use the same form of a gravitational potential as expressed in Eq(2) in order to find acceleration due to gravity at various points on the surface of the planet.

References

1. "Planetary Orbits as Simple Harmonic Motion." Resonance, vol. 8, no. 12, Dec. 2003, pp. 83–91. https://doi.org/10.1007/bf02839055.s.ac.in/article/fulltext/reso/008/12/0083-0091

2. Rozelot, J. P., et al. "A Brief History of the Solar Oblateness. A Review." Journal of Atmospheric and Solar-Terrestrial Physics, vol. 73, no. 2–3, Feb. 2011, pp. 241–50. https://doi.org/10.1016/j.jastp.2010.02.021.

3. Irbah, Abdanour, et al. "Variations of Solar Oblateness With the 22 Yr Magnetic Cycle Explain Apparently Inconsistent Measurements." The Astrophysical Journal, vol. 875, no. 2, American Astronomical Society, Apr. 2019, p. L26. https://doi.org/10.3847/2041-8213/ab16e2.

Appendix

The python notebook used for this project can be found here.